World Journal of Gastroenterology

Submit a Manuscript: http://www.wjgnet.com/esps/
Help Desk: http://www.wjgnet.com/esps/helpdesk.aspx
DOI: 10.3748/wjg.v21.i25.7824

World J Gastroenterol 2015 July 7; 21(25): 7824-7833
ISSN 1007-9327 (print) ISSN 2219-2840 (online)

ORIGINAL ARTICLE

Retrospective Study

Gd-EOB-DTPA-enhanced magnetic resonance imaging for bile duct intraductal papillary mucinous neoplasms

Shi-Hong Ying, Xiao-Dong Teng, Zhao-Ming Wang, Qi-Dong Wang, Yi-Lei Zhao, Feng Chen, Wen-Bo Xiao

Shi-Hong Ying, Qi-Dong Wang, Yi-Lei Zhao, Feng Chen, Wen-Bo Xiao, Department of Radiology, The First Affiliated Hospital, College of Medicine, Zhejiang University, Hangzhou 310003, Zhejiang Province, China

Xiao-Dong Teng, Zhao-Ming Wang, Department of Pathology, The First Affiliated Hospital, College of Medicine, Zhejiang University, Hangzhou 310003, Zhejiang Province, China

Author contributions: Ying SH, Chen F and Xiao WB designed the research; Ying SH, Teng XD and Wang QD performed the research; Wang ZM and Zhao YL analyzed the data; Ying SH, Chen F and Xiao WB wrote the paper; all authors approved the final version for publication.

Supported by National Natural Science Foundation of China, No. 81171388; and Ministry of Health Research Foundation of China (in part), No. WKJ2011-2-004.

Ethics approval: The study was a retrospective study, and every patient had undergone ethoxybenzyl-enhanced magnetic resonance imaging according to clinical routine.

Informed consent statement: Informed written consent was obtained from all patients.

Conflict-of-interest statement: Authors have no conflicts of interest for this paper.

Data sharing statement: No additional data are available.

Correspondence to: Wen-Bo Xiao, MD, Chief Doctor, Department of Radiology, The First Affiliated Hospital, College of Medicine, Zhejiang University, No. 79 Qingchun Road, Hangzhou 310003, Zhejiang Province, China. xiaowb.111@163.com
Telephone: +86-571-87236587
Fax: +86-571-87236587

Received: December 14, 2014
Peer-review started: December 18, 2014
First decision: January 22, 2015
Revised: February 20, 2015
Accepted: April 17, 2015
Article in press: April 17, 2015
Published online: July 7, 2015

Abstract

AIM: To investigate gadolinium-ethoxybenzyl-diethylenetriamine-pentaacetic acid (Gd-EOB-DTPA)-enhanced magnetic resonance imaging (MRI) of intraductal papillary mucinous neoplasms of the bile duct (IPMN-B).

METHODS: The imaging findings of five cases of IPMN-B which were pathologically confirmed at our hospital between March 2012 and May 2013 were retrospectively analyzed. Three of these cases were diagnosed by duodenal endoscopy and biopsy pathology, and two cases were diagnosed by surgical pathology. All five patients underwent enhanced and non-enhanced computed tomography (CT), magnetic resonance cholangiopancreatography, and Gd-EOB-DTPA-enhanced MRI; one case underwent both Gd-EOB-DTPA-enhanced MRI and positron emission tomography-CT. The clinical data and imaging results for these cases were compared and are presented.

RESULTS: Conventional imaging showed diffuse

dilatation of bile ducts and multiple intraductal polypoid and papillary neoplasms or serrated changes along the bile ducts. In two cases, Gd-EOB-DTPA-enhanced MRI revealed dilated biliary ducts and intraductal tumors, as well as filling defects caused by mucin in the dilated bile ducts in the hepatobiliary phase. Gd-EOB-DTPA-enhanced MRI in one case clearly showed a low-signal tumor in the hepatobiliary phase, similar to what was seen by positron emission tomography-CT. In two patients, routine inspection was unable to discern whether the lesions were inflammation or tumors. However, Gd-EOB-DTPA-enhanced MRI revealed a pattern of gradual enhancement during the hepatobiliary phase, and the signal intensity of the lesions was lower than the surrounding liver parenchyma, suggesting tissue inflammation in both cases, which were confirmed by surgical pathology.

CONCLUSION: Gd-EOB-DTPA-enhanced MRI reveals the intraductal mucin component of IPMN-B in some cases and the extent of tumor infiltration beyond the bile ducts in invasive cases.

Key words: Gadolinium-ethoxybenzyl-diethylenetriamine pentaacetic acid; Magnetic resonance imaging; Magnetic resonance cholangiopancreatography; Multidetector computed tomography; Bile duct neoplasms

Core tip: Gadolinium-ethoxybenzyl-diethylenetriamine-pentaacetic acid (Gd-EOB-DTPA)-enhanced magnetic resonance imaging (MRI) can be used to demonstrate the filling defects due to mucin secreted by intraductal papillary mucinous neoplasms of the bile duct (IPMN-B) and to display the extent of tumor infiltration beyond bile ducts in cases with invasive IPMN-B. It also has the potential to differentiate tumor tissue from inflammatory lesions. Therefore, Gd-EOB-DTPA-enhanced MRI may improve the clinical management of IPMN-B.

Ying SH, Teng XD, Wang ZM, Wang QD, Zhao YL, Chen F, Xiao WB. Gd-EOB-DTPA-enhanced magnetic resonance imaging for bile duct intraductal papillary mucinous neoplasms. *World J Gastroenterol* 2015; 21(25): 7824-7833 Available from: URL: http://www.wjgnet.com/1007-9327/full/v21/i25/7824.htm DOI: http://dx.doi.org/10.3748/wjg.v21.i25.7824

INTRODUCTION

Intraductal papillary mucinous neoplasms of the bile duct (IPMN-B) are a subtype of intraductal papillary neoplasms of the bile duct with macroscopically visible mucin secretion[1-7]. The clinical manifestations, histopathologic features, and immunohistochemical and biologic behaviors of this bile duct subtype are similar to IPMNs of the pancreas[1-6]. IPMN-B originates from biliary epithelial cells, and can be pathologically defined as papillary adenoma, papillomatosis, carcinoma *in situ*, or invasive adenocarcinoma. Imaging findings of IPMN-B include: papillary or polypoid growth of the tumor along the bile duct or serrated inner lining of the bile duct; expansive and significant dilation of the bile duct upstream and downstream of the tumor; or aneurysmal dilation of the bile duct at the site of the tumor[8-10]. However, confirmation of a diagnosis requires the use of endoscopic retrograde cholangiopancreatography (ERCP) to determine the presence of mucin secreted by the tumor[4]. In addition, malignant IPMN-Bs can invade the liver and form a mass, although conventional ultrasonography (US), computed tomography (CT), and dynamic enhancement magnetic resonance scans cannot define the scope of tumor invasion, or distinguish the accompanying inflammation from the tumor[11,12].

Gadolinium-ethoxybenzyl-diethylenetriamine pentaacetic acid (Gd-EOB-DTPA) is a double-specific contrast agent that provides enhancement effects similar to Gd-DTPA in dynamic enhanced scans. With Gd-EOB-DTPA, 50% of the contrast injection is absorbed by hepatocytes and drained *via* the bile duct in the hepatobiliary phase. Although this contrast agent has been used for the diagnosis of hepatogenic tumor lesions[11], only two reports (four cases) describe the use of Gd-EOB-DTPA-enhanced magnetic resonance imaging (MRI) for the diagnosis of IPMN-B[13,14]. In those reports, Gd-EOB-DTPA-enhanced MRI not only revealed the dilated bile duct and the enhanced tumor tissues within it, but also confirmed that the filling defect of the bile duct at the hepatobiliary phase was mucus secreted by the tumors[13,14], thus demonstrating its unique value for tumor diagnosis. The present study describes the application of Gd-EOB-DTPA-enhanced MRI in five cases of IPMN-B. In addition to displaying the features of IPMN-Bs, this method reveals the extent of invasion into the extrahepatic bile duct in malignant cases. Furthermore, Gd-EOB-DTPA-enhanced MRI can discern tumor tissue from surrounding inflammation, which has not previously been reported.

MATERIALS AND METHODS

Study subjects

Five cases of IPMN-B in our hospital during the period from March 2012 to May 2013 were retrospectively analyzed (Table 1). Two cases were confirmed by surgical pathology. Three cases underwent thick-needle biopsy, and 3-5 pieces of cord-like tissue were obtained for each case; diagnoses were confirmed by two senior pathologists.

Table 1 Clinical data of five patients with intraductal papillary mucinous neoplasms of the bile duct

No.	Sex	Age (yr)	History and symptoms	Laboratory findings (normal range)	Imaging						
					US	CT + C	Gd-DTPA MRI	MRCP	ERCP	PET-CT	Gd-EOB-DTPA-enhanced MRI
1	Female	59	Recurrent upper abdominal pain with nausea and vomiting for 6 mo	No significant abnormalities	A	A	NA	A	A	NA	A
2	Male	52	Physical examination revealed liver tumor	CEA: 7.5 ng/mL (0.0-8.0)	A	A	NA	A	A	NA	A
3	Female	72	Jaundice	CEA: 9.8 ng/mL CA199: 715.1 U/mL (0.0-37.0) Total bilirubin: 611 mmol/L (0-21)	A	A	NA	A	A	NA	A
4	Male	66	Jaundice	CEA: 44.0 ng/mL CA199: > 12000 U/mL Total bilirubin: 424 mmol/L	A	A	NA	A	NA	NA	A
5	Male	56	8-yr history of liver contusion; liver pain for 6 mo	CA199: 217.3 U/mL CRP: 34.5 mg/L (0.0-8.0)	A	A	A	A	NA	A	A

A: Applied; CA: Cancer antigen; CEA: Carcinoembryonic antigen; CRP: C-reactive protein; CT + C: Contrast enhanced-CT; ERCP: Endoscopic retrograde cholangiopancreatography; Gd-DTPA MRI: Gadolinium-diethylenetriamine pentaacetic acid magnetic resonance imaging; Gd-EOB-DTPA-enhanced MRI: Gadolinium-ethoxybenzyl-diethylenetriamine-pentaacetic acid-enhanced magnetic resonance imaging; MRCP: Magnetic resonance cholangiopancreatography; NA: Not applied; PET: Positron emission tomography; US: Ultrasound.

Hepatic CT examinations

CT images were acquired by a 16-slice CT scanner (Aquilion; Toshiba, Tokyo, Japan) using the following scan parameters: 120 kV; 250 mA; reconstruction thickness, 5 mm; layer spacing, 5 mm. CT scans were obtained before and after intravenous administration of 80-100 mL contrast agent (300 mg I/mL Ultravist; Bayer Healthcare, Berlin, Germany) at a speed of 3.0 mL/s. CT scan delays after the injection of contrast agent were 25-30 s, 65 s, and 120 s for the arterial, portal venous, and delayed phases, respectively.

Hepatic MRI examinations

MRI was performed using a 3.0 T scanner (Signa HDxt 3.0 T; GE Healthcare, Little Chalfont, United Kingdom) with a corresponding eight-channel phase-array abdomen coil system. MRI sequences included axial T2- and diffusion-weighted imaging, magnetic resonance cholangiopancreatography (MRCP) and fat suppression T1-weighted three-dimensional liver acquisition with volume acceleration (LAVA)-enhanced imaging. The parameters for MRI sequences used in this study are listed in Table 2.

The LAVA-enhanced MRI was conducted *via* bolus i.v. injection of Gd-DPTA (Magnevist; Schering, Berlin, Germany) at 0.1 mmol/kg body weight and a speed of 2 mL/s. Pre-contrast and dynamic contrast-enhanced multi-phase MRI scans were acquired. The MRI scan delays were 25-30 s, 85 s, and 180 s for the arterial, portal venous, and delayed phases, respectively. The same sequence and parameters were used for dynamic Gd-EOB-DPTA-enhanced MRI following a bolus i.v. injection of EOB (Primovist; Bayer Healthcare) at 0.025 mmol/kg body weight and a speed of 2 mL/s. Fat suppression T1-weighted three-dimensional LAVA was performed 20 min after contrast injection and the images of the initial hepatobiliary phase were obtained, and repeated after 42-52 min for the delayed scans of the hepatobiliary phase. The image of the hepatobiliary phase was visualized with maximum intensity projections or multiple planar reconstructions to observe the filling condition of the intra- and extrahepatic bile ducts[11,12,15].

US and PET-CT

All US studies were performed using a color ultrasound (Sequoia 512; Siemens Medical Solutions, Munich, Germany) with a 1.0- to 4.0-MHz convex probe. One patient received a whole-body PET/CT scan performed on an integrated PET/CT scanner (Biograph 16; Siemens Medical Solutions) after the injection of 350 MBq 18F-FDG.

RESULTS

General imaging findings

US, CT/MRI, and MRCP depicted extensive intra- and extrahepatic bile duct dilatation in cases 1-4, including upstream and downstream of the tumor and at the segmental bile duct (Figures 1, 2, 3 and 4). In contrast-enhanced CT and MRI examinations, multiple polypoid or papillary tumors which were distributed along the bile ducts showed mild to medium enhancement. In case 2, partial right intrahepatic bile ducts were seen as aneurysm-like dilatations (Figure 2). In case 4, a slightly higher-signal nodule was also

Table 2 Parameters for magnetic resonance imaging sequences

Sequence	TR (ms)	TE (ms)	Section thickness (mm)	Gap (mm)	Matrix size (pixels)	Flip angle (degrees)	Field of view (cm)
T2WI	6000-10000	91	6	2	320 × 224	90	40 × 32
DWI (b = 1000)	8000	65	6	2	128 × 128	90	40 × 32
MRCP	6000-10000	800	2.4	0	384 × 224	90	40 × 32
Gd-DTPA-enhanced MRI	2.84	1.34	5	0	384 × 256	10	40 × 32
Gd-EOB-DTPA-enhanced MRI	2.84	1.34	5	0	384 × 256	10	40 × 32

DWI: Diffusion-weighted imaging; DTPA: Diethylenetriamine pentaacetic acid; EOB: Ethoxybenzyl; Gd: Gadolinium; MRCP: Magnetic resonance cholangiopancreatography; MRI: Magnetic resonance imaging; T2WI: T2-weighted imaging; TE: Echo time; TR: Repetition time.

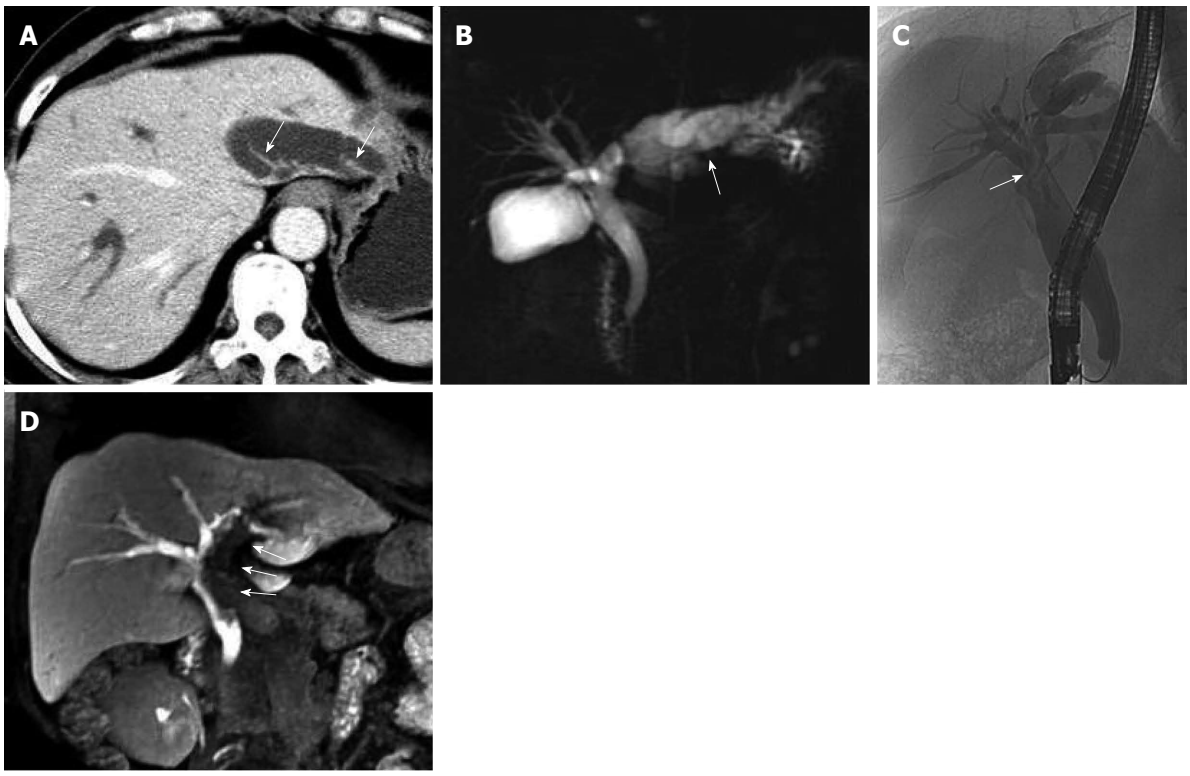

Figure 1 Fifty-nine-year-old female patient with intraductal papillary mucinous neoplasm of the bile duct (case 1). A: Axial contrast-enhanced computed tomography in the portal phase; B: Magnetic resonance cholangiopancreatography showed extensive intra- and extrahepatic bile duct dilatation and multiple hydra-like protrusions (arrows) in the markedly dilated left intrahepatic bile duct (arrow); C: Endoscopic retrograde cholangiopancreatography showed extensive intra- and extrahepatic bile duct dilatation, particularly in the left intrahepatic and common bile ducts. Bile ducts in the liver hilar appeared more transparent due to the local aggregation of mucin (arrow); D: Multiple planar reconstruction of gadolinium-ethoxybenzyl-diethylenetriamine-pentaacetic acid-enhanced magnetic resonance imaging in the hepatobiliary phase showed dilatation of the bile duct and filling defects in the left intrahepatic and common bile ducts, with a cup-shaped contrast filling edge (arrows). The filling defects were caused by mucus retention, which was confirmed by endoscopy.

seen at the edge of the dilated left intrahepatic bile ducts in T2- and diffusion-weighted imaging, which was enhanced slightly during all three phases of the contrast-enhanced CT scan (Figure 4). In this case, the tumor lesions were considered to penetrate into the liver *via* the bile duct wall. In case 5, CT/MRI scans depicted right hepatic atrophy surrounding the right dilated intrahepatic bile duct (Figure 5). Enhanced CT and Gd-DPTA-enhanced MRI in both the arterial and portal venous phases depicted marked, although ill-defined, patchy enhancement around the dilated bile duct, which was isodense in the delayed phase. Positron emission tomography (PET)-CT in case 5 revealed a mass of 6.5 cm × 6.0 cm with high uptake of fluorodeoxyglucose (FDG) around the dilated bile duct in the posterior segment of the liver (the maximum standard uptake value was 6.5), indicating a malignant tumor (Figure 5). Therefore, the tumor in this patient was considered to be an invasive IPMN-B.

Gd-EOB-DTPA-enhanced MRI

Dilated bile ducts and tumors on the bile duct walls in the five cases were also observed with plain MRI and dynamic triple-enhanced EOB scans. In addition, some specific signs were seen in ⩾ 20 min delayed scans, namely the hepatobiliary phase. Cases 1 and 2 showed irregular columnar filling defects, and the edge of the contrast reagent appeared in a cupped or half-

Figure 2 Fifty-two-year-old male patient with cystic intraductal papillary mucinous neoplasm of the bile duct (case 2). A: Coronal image of contrast-enhanced computed tomography; B: Gadolinium-ethoxybenzyl-diethylenetriamine-pentaacetic acid-enhanced magnetic resonance imaging (Gd-EOB-DTPA-enhanced MRI) in the portal venous phase showed extensive biliary and aneurysmal dilatations of the right intrahepatic bile duct, with multiple significantly enhanced masses within the lumen (black arrows); C: Gd-EOB-DTPA-enhanced MRI also showed a contrast-filling defect within the common bile duct (white arrows), suggesting the presence of mucin; D: Multiple planar reconstruction of images acquired in the hepatobiliary phase showed a dilated left intrahepatic bile duct with good contrast filling (black arrows). The contrast filling was incomplete in the right intrahepatic and common bile ducts (white arrows).

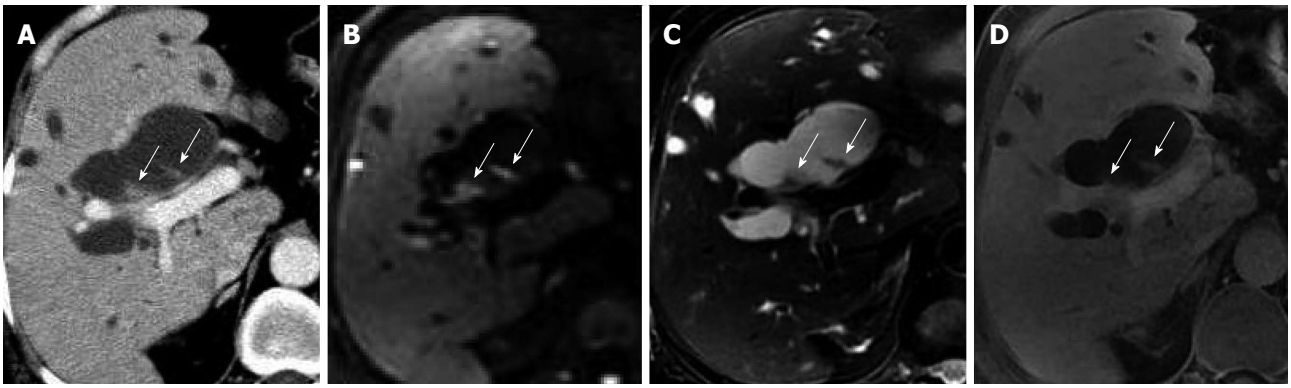

Figure 3 Seventy-two-year-old female patient with malignant intraductal papillary mucinous neoplasm of the bile duct (case 3). A: Axial image of enhanced computed tomography in the portal venous phase showed extensive intra- and extrahepatic bile duct dilatation with multiple hydra-like protrusions (arrows); B: Dilation appeared hyperintense (arrows) with diffusion-weighted imaging; C: Hypointense (arrows) with T2-weighted imaging; D: Gadolinium-ethoxybenzyl-diethylenetriamine-pentaacetic acid-enhanced magnetic resonance imaging in the hepatobiliary phase revealed no hyperintense bile with distribution of the contrast agents in the dilated bile duct, indicating a large amount of mucin retention, which was confirmed by endoscopy.

ring distribution (Figures 1 and 2).

Cholangiectasis was apparent in cases 3 and 4, and a high signal of contrast filling was not seen in the dilated bile ducts in the hepatobiliary phase (Figures 3 and 4). Total bilirubin levels were markedly elevated in these two cases (Table 1). Routine inspection showed an abnormal signal and low-strengthened focal area in the edge of the left intrahepatic bile duct in case 4, and the edge of the lesion was enhanced in the 20-min delayed EOB-enhanced MRI. In the 45-min delayed scan, most of the area showed isointensity, with the exception of the low signal in the lesion center, which is a pattern of gradual enhancement (Figure 4). These findings suggest decreased hepatic uptake of contrast agent, indicative of inflammation. No signs of tumor invasion were seen in the EOB-enhanced scans of

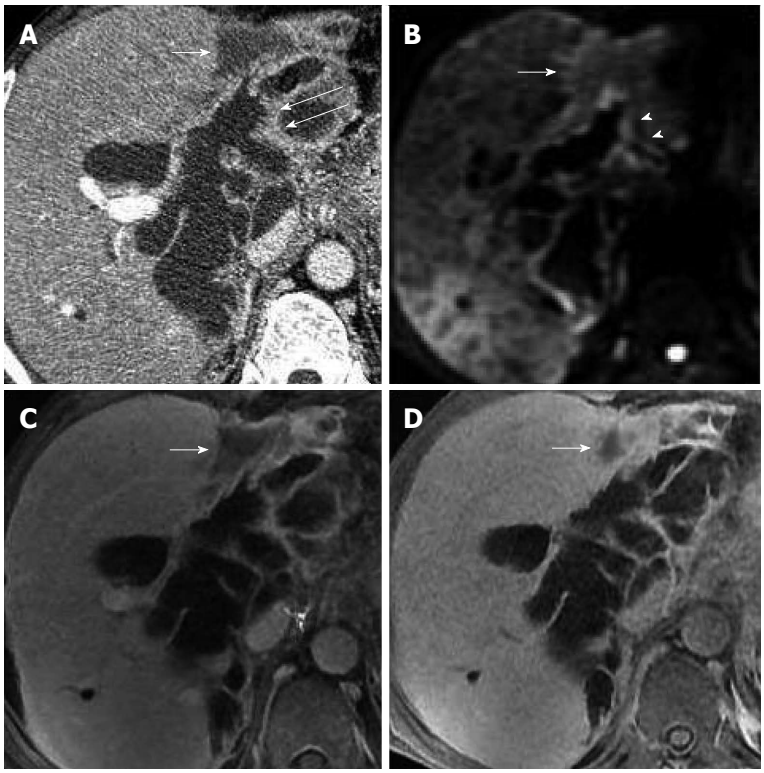

Figure 4 Sixty-six-year-old male patient with malignant intraductal papillary mucinous neoplasm of the bile duct (case 4). A: Axial image of contrast-enhanced computed tomography in the portal venous phase showed a patchy hypointense area abutting the dilated bile ducts in the front edge of the left liver lobe (white arrow), and multiple small nodules distributed along the bile duct wall within the lumen (white long arrows); B: These nodules were hyperintense (white arrowheads) with diffusion-weighted imaging; C: Gadolinium-ethoxybenzyl-diethylenetriamine-pentaacetic acid-enhanced magnetic resonance imaging (Gd-EOB-DTPA-enhanced MRI) in the portal venous phase also showed a patchy hypointense area abutting the dilated bile ducts (white arrow); D: The patch (white arrow) appeared smaller with Gd-EOB-DTPA-enhanced MRI in the hepatobiliary phase, due to the gradual filling of contrast agent, which suggests the presence of functional liver cells. The patchy area was thought to be an inflammatory change secondary to the tumor.

cases 1-4.

Although there was no high signal of contrast filling in the dilated bile duct on the inferior right liver in case 5, the 20-min delayed scan showed a well-defined massive (6.5 cm × 6.0 cm) lesion with low-signal intensity around the dilated bile duct, indicating a lack of EOB uptake in the adjacent region of the liver (Figure 5). This was in accordance with the tumor extent seen on PET-CT. The signal in the liver parenchyma in front of the tumor was slightly lower than the normal liver tissue, but higher than the mass tissue in the hepatobiliary phase of EOB-enhanced MRI. A low signal vessel with normal direction can be seen within it, suggesting that this area is not tumor tissue, but inflamed liver tissue with reduced uptake ability for the contrast agent (Figure 5).

Pathology and treatment

Cases 1-3 underwent duodenal endoscopy to drain mucus from the duodenal papilla within 3 d. In case 4, EOB-enhanced MRI showed tumor distribution in the left and right hepatic ducts, but no signs of extra-biliary tumor invasion, therefore, biliary tumor enucleation and T tube drainage were performed. During the procedure, the dilated bile duct was filled with mucus, and multiple nodular or papillary tumors were observed in the bile duct.

Microscopic examination of the biopsies from cases 1-4 showed cuboidal or columnar epithelial cells around the fibers and vessels growing within the bile duct, with no tumor invasion beyond the bile duct. Immunohistochemical results were: mucin (MUC)1$^-$, MUC2$^+$, MUC5AC$^+$, MUC6$^-$, and p53$^-$.

Based on the findings from imaging, endoscopy, and biopsy or surgical pathology, cases 1 and 3 were pathologically diagnosed as papillary adenoma, and cases 2 and 4, which showed obvious tumor nuclear atypia in the focal lesions, were diagnosed as papillary adenoma accompanied by focal cancer. In case 4, lesions beyond the left dilated bile duct were removed, and the pathology showed infiltration of inflammatory cells without tumor cells, thus, these were diagnosed as inflammatory lesions. Lesions in cases 1 and 2 were confined to the left or right lobe, suggesting lobe resection, although the patients refused surgery. Case 3 involved the left and right intrahepatic bile ducts and lobe resection could not be performed. Hence, cases 1-3 underwent endoscopic nasobiliary drainage and/or percutaneous transhepatic cholangial drainage to alleviate the symptoms.

Case 5 underwent a right hepatic resection. The EOB-enhanced MRI indicated that the anterior right

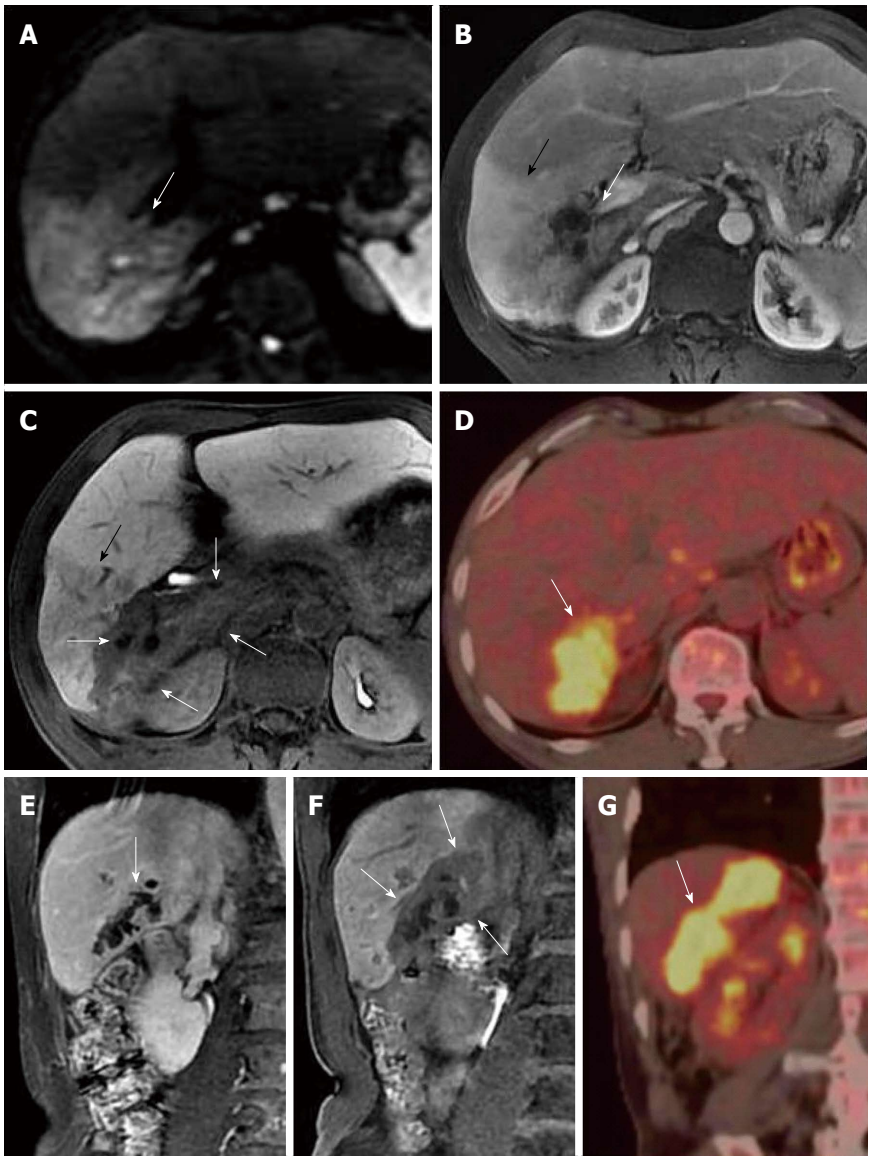

Figure 5 Fifty-six-year-old male patient with infiltrative intraductal papillary mucinous neoplasm of the bile duct (case 5). A: Diffusion-weighted imaging showed a hyperintense area in segment VI of the liver (white arrow); B: Gadolinium (Gd)-diethylenetriamine-pentaacetic acid (DTPA)-enhanced magnetic resonance imaging (MRI) in the portal venous phase showed marked enhancement in the anterior subsegment (black arrow) and a slightly hypointense area in the posterior subsegment of segment Ⅵ (white arrow); C: Gd-ethoxybenzyl (EOB)- -DTPA-enhanced MRI in the hepatobiliary phase revealed bile duct dilatation in the posterior subsegment of segment Ⅵ without contrast filling. The hypointense area around the dilated bile duct indicated tumor infiltration to the surrounding tissue (white arrows). The anterior subsegment of segment Ⅵ with a slightly decreased low signal intensity suggested an inflammatory change (black arrow); D: Positron emission tomography-computed tomography (CT) confirmed the tumor in the posterior subsegment of segment Ⅵ with substantial uptake of fluorodeoxyglucose (white arrow), suggesting active tumor metabolism; E: Coronal Gd-DTPA-enhanced MRI in the equilibrium phase showed serrated changes in the bile duct wall of the posterior subsegment of segment Ⅵ, and the extra-biliary tumor infiltration was not well identified (white arrow); F: Gd-EOB-DTPA-enhanced MRI in the hepatobiliary phase showed bile duct dilatation in the posterior subsegment of segment Ⅵ without contrast filling. The tumor infiltration surrounding the dilated bile duct was hypointense and well defined (white arrows); G: Fluorodeoxyglucose uptake by the tumor (white arrow) was also shown in the posterior subsegment of segment Ⅵ during positron emission tomography-CT.

liver was inflamed, so the middle hepatic vein was completely retained. During surgery, a mass (6.5 cm × 6.5 cm × 6.0 cm) was seen in the posterior right liver, showing extra-biliary infiltration with dilated bile ducts filling with mucus. Postoperative pathology showed cuboidal or columnar epithelial cells in the tumor tissues growing around the fibers and vessels inside the bile duct. The tumor cells had obvious nuclear atypia, which invaded outward to the bile duct wall. Immunohistochemistry showed that the cells were MUC1$^+$, MUC2$^+$, MUC5AC$^+$, MUC6$^-$, and p53$^+$, confirming the diagnosis of infiltrating intraductal papillary mucinous adenocarcinoma of the bile duct. The right anterior liver parenchyma showed interstitial fibrous tissue hyperplasia with chronic inflammatory cell infiltration, which was diagnosed as chronic

inflammation with fibrous tissue hyperplasia.

DISCUSSION

Surgery is the preferred treatment for IPMN-B. Partial hepatectomy can be performed for localized tumors, whereas bilateral bile duct involvement may require liver transplantation, duodenal papilla dissection, endoscopic nasobiliary drainage, and/or percutaneous transhepatic cholangial drainage[16-19]. Biliary tumor enucleation can be performed for tumors that do not invade into the bile duct[6,20-23]. Thus, accurate preoperative diagnosis, with determination of the extent of tumor involvement, is crucial for treatment decisions.

Reports by Lim *et al*[8-10] describe the typical imaging findings of IPMN-B. The disease can be clearly diagnosed when imaging findings are indicative of IPMN-B, and the presence of mucin within the dilated bile duct is confirmed. Although duodenal endoscopy, ERCP, biliary tract endoscopy, and endoscopic US can be used to clearly identify the tumor and mucus[13,24-27], these are invasive examinations, the success of which is associated with the proficiency of the operator, and are accompanied by a risk of pancreatitis. Moreover, it is difficult to evaluate upstream of the bile duct obstruction and extra-biliary conditions with these methods[28-30].

Takanami *et al*[13] and Oki *et al*[14] used EOB-enhanced MRI to study four patients with IPMN-B, and found that Gd-EOB-DTPA-enhanced MRI shows the dilated bile duct and tumor, but also the bile duct filling defects caused by mucin retention. Therefore, Gd-EOB-DTPA-enhanced MRI is an alternative to ERCP for the diagnosis of IPMN-B. Indeed, the performance of EOB-enhanced MRI in cases 1 and 2 in the present study is in agreement with the previous reports[13,14]. Although biliary sludge and stones can also appear as filling defects in EOB-enhanced MRI, they show a low signal in T2-weighted images that can be differentiated from mucus, as shown in cases 1 and 2. Although the cystic appearance of the IPMN-B in case 2 is similar to cystadenoma or cystadenocarcinoma, these cystic lesions are not connected with the bile duct. Moreover, contrast agent was seen in both the cystic lesion and the bile duct in case 2 during the hepatobiliary phase of Gd-EOB-DTPA-enhanced MRI.

A large amount of mucin in the bile duct was confirmed during ERCP/operation in cases 3 and 4, which resulted in marked bile duct dilatation and obvious impaired liver function (indicated by elevated total bilirubin levels). Furthermore, liver cell uptake and secretion of EOB into the bile duct was obviously decreased, with none observed in the hepatobiliary phase in the 42-52-min delayed scan. Mucin within the bile duct can be distinguished from bile based on the similarity with signals in the downstream bile duct, lobe, or segmental bile duct where the tumor is not located.

Case 4 showed a long T2-signal nodule with hypo-enhancement at the edge of the left intrahepatic bile duct, which was considered to be focal. However, EOB-enhanced imaging during the hepatobiliary phase showed gradual enhancement of the lesion area, consistent with chronic inflammation. Therefore, the patient underwent biliary tumor enucleation and T tube drainage, a procedure that could accelerate the disease if the tumor had invaded tissue outside of the bile duct. Therefore, when multifocal IPMN-B occurs in intrahepatic bile ducts, EOB-enhanced MRI in the hepatobiliary phase can be used to select the appropriate treatment.

Importantly, case 5 describes imaging results from an invasive IPMN-B, which cannot be discerned with conventional-enhanced CT or Gd-DTPA-enhanced MRI[1,6,16]. With similar cases, it is difficult to judge the extent of tumor invasion into the extrahepatic bile duct by routine inspection, as demonstrated in this patient. The extent of the infringement was clear by PET-CT examination, and the FDG uptake suggested that the tumor was malignant, although it is difficult to distinguish this tumor type from cholangiocarcinoma and other malignant liver tumors. Takanami *et al*[31] also reported PET-CT manifestations of invasive IPMN-B, observed as high intake of FDG. Despite its advantage, PET-CT should be used very carefully due to the relatively high cost and risk of radioactive damage to patients. Case 5 further demonstrates that normal liver cells uptake Gd-EOB-DTPA, whereas tumor cells do not, thus more clearly defining the extent of liver invasion. Moreover, case 5 shows that the signal intensity of the right anterior liver in the hepatobiliary phase is intermediate between normal liver parenchyma and tumor, representing the nature of inflammatory tissue with decreased liver function (EOB uptake). In this case, the tumor, inflammation, and normal liver tissues were clearly demarcated, thus we decided to retain the middle hepatic vein during the right liver resection, and were confident in the negative cut edge of the tumor.

In conclusion, patients with suspected IPMN-B based on imaging findings would benefit from EOB-enhanced MRI for determination of the presence of mucus and extent of extra-biliary invasion.

COMMENTS

Background

Reports and awareness of intraductal papillary mucinous neoplasm of the bile duct (IPMN-B) are increasing. However, difficulties remain with noninvasive methods for diagnosis and determining the extent of the tumor.

Research frontiers

This study reports the use of a novel imaging technique, gadolinium-ethoxybenzyl-diethylenetriamine-pentaacetic acid (Gd-EOB-DTPA)-enhanced magnetic resonance imaging (MRI), for diagnosing IPMN-B.

Innovations and breakthroughs

This study shows that Gd-EOB-DTPA-enhanced MRI can reveal bile duct filling defects due to mucin, which is highly suggestive of a diagnosis for IPMN-B. Compared with positron emission tomography-computed tomography, Gd-EOB-

DTPA-enhanced MRI can be used to differentiate inflammatory lesions from tumor tissue. Therefore, Gd-EOB-DTPA-enhanced MRI facilitates accurate diagnosis and proper management of IPMN-B.

Applications

EOB-enhanced MRI is a useful, noninvasive method to detect mucus and assess the extent of extra-biliary invasion in patients whose imaging findings indicate IPMN-B.

Terminology

Gd-EOB-DTPA is a double-specific contrast agent that is absorbed by hepatocytes and drained *via* the bile duct in the hepatobiliary phase, and can be used to detect filling defects due to mucus. It can also be used to distinguish between tumor cells, which do not take up the contrast agent, and inflammatory cells, which show reduced signal intensity compared to normal liver tissue.

Peer-review

This is an interesting case series of patients with IPMN-B, in which Gd-EOB-DTPA-enhanced MRI was applied for better evaluation of the lesion and differentiation between tumor invasion and inflammation.

REFERENCES

1 **Zen Y**, Fujii T, Itatsu K, Nakamura K, Minato H, Kasashima S, Kurumaya H, Katayanagi K, Kawashima A, Masuda S, Niwa H, Mitsui T, Asada Y, Miura S, Ohta T, Nakanuma Y. Biliary papillary tumors share pathological features with intraductal papillary mucinous neoplasm of the pancreas. *Hepatology* 2006; **44**: 1333-1343 [PMID: 17058219 DOI: 10.1002/hep.21387]

2 **Ohtsuka M**, Kimura F, Shimizu H, Yoshidome H, Kato A, Yoshitomi H, Furukawa K, Takeuchi D, Takayashiki T, Suda K, Takano S, Kondo Y, Miyazaki M. Similarities and differences between intraductal papillary tumors of the bile duct with and without macroscopically visible mucin secretion. *Am J Surg Pathol* 2011; **35**: 512-521 [PMID: 21412069 DOI: 10.1097/PAS.0b013e3182103f36]

3 **Nakanuma Y**. A novel approach to biliary tract pathology based on similarities to pancreatic counterparts: is the biliary tract an incomplete pancreas? *Pathol Int* 2010; **60**: 419-429 [PMID: 20518896 DOI: 10.1111/j.1440-1827.2010.02543.x]

4 **Yeh TS**, Tseng JH, Chen TC, Liu NJ, Chiu CT, Jan YY, Chen MF. Characterization of intrahepatic cholangiocarcinoma of the intraductal growth-type and its precursor lesions. *Hepatology* 2005; **42**: 657-664 [PMID: 16116640 DOI: 10.1002/hep.20837]

5 **D'souza MA**, Isaksson B, Löhr M, Enochsson L, Swahn F, Lundell L, Arnelo U. The clinicopathological spectrum and management of intraductal papillary mucinous neoplasm of the bile duct (IPMN-B). *Scand J Gastroenterol* 2013; **48**: 473-479 [PMID: 23330596 DOI: 10.3109/00365521.2012.722672]

6 **Rocha FG**, Lee H, Katabi N, DeMatteo RP, Fong Y, D'Angelica MI, Allen PJ, Klimstra DS, Jarnagin WR. Intraductal papillary neoplasm of the bile duct: a biliary equivalent to intraductal papillary mucinous neoplasm of the pancreas? *Hepatology* 2012; **56**: 1352-1360 [PMID: 22504729 DOI: 10.1002/hep.25786]

7 **Klibansky DA**, Reid-Lombardo KM, Gordon SR, Gardner TB. The clinical relevance of the increasing incidence of intraductal papillary mucinous neoplasm. *Clin Gastroenterol Hepatol* 2012; **10**: 555-558 [PMID: 22210438 DOI: 10.1016/j.cgh.2011.12.029]

8 **Lim JH**, Yoon KH, Kim SH, Kim HY, Lim HK, Song SY, Nam KJ. Intraductal papillary mucinous tumor of the bile ducts. *Radiographics* 2004; **24**: 53-66; discussion 66-67 [PMID: 14730036 DOI: 10.1148/rg.241035002]

9 **Lim JH**, Jang KT, Choi D. Biliary intraductal papillary-mucinous neoplasm manifesting only as dilatation of the hepatic lobar or segmental bile ducts: imaging features in six patients. *AJR Am J Roentgenol* 2008; **191**: 778-782 [PMID: 18716109 DOI: 10.2214/AJR.07.2091]

10 **Lim JH**, Jang KT, Rhim H, Kim YS, Lee KT, Choi SH. Biliary cystic intraductal papillary mucinous tumor and cystadenoma/cystadenocarcinoma: differentiation by CT. *Abdom Imaging* 2007; **32**: 644-651 [PMID: 17437076 DOI: 10.1007/s00261-006-9161-5]

11 **Van Beers BE**, Pastor CM, Hussain HK. Primovist, Eovist: what to expect? *J Hepatol* 2012; **57**: 421-429 [PMID: 22504332 DOI: 10.1016/j.jhep.2012.01.031]

12 **Seale MK**, Catalano OA, Saini S, Hahn PF, Sahani DV. Hepatobiliary-specific MR contrast agents: role in imaging the liver and biliary tree. *Radiographics* 2009; **29**: 1725-1748 [PMID: 19959518 DOI: 10.1148/rg.296095515]

13 **Takanami K**, Yamada T, Tsuda M, Takase K, Ishida K, Nakamura Y, Kanno A, Shimosegawa T, Unno M, Takahashi S. Intraductal papillary mucininous neoplasm of the bile ducts: multimodality assessment with pathologic correlation. *Abdom Imaging* 2011; **36**: 447-456 [PMID: 20959978 DOI: 10.1007/s00261-010-9649-x]

14 **Oki H**, Hayashida Y, Namimoto T, Aoki T, Korogi Y, Yamashita Y. Usefulness of gadolinium-ethoxybenzyl-diethylenetriamine pentaacetic acid-enhanced magnetic resonance cholangiography for detecting mucin retention in bile ducts: a rare intraductal papillary mucinous neoplasm of the bile duct. *Jpn J Radiol* 2011; **29**: 590-594 [PMID: 21928003 DOI: 10.1007/s11604-011-0593-7]

15 **Lee NK**, Kim S, Lee JW, Lee SH, Kang DH, Kim GH, Seo HI. Biliary MR imaging with Gd-EOB-DTPA and its clinical applications. *Radiographics* 2009; **29**: 1707-1724 [PMID: 19959517 DOI: 10.1148/rg.296095501]

16 **Budzynska A**, Hartleb M, Nowakowska-Dulawa E, Krol R, Remiszewski P, Mazurkiewicz M. Simultaneous liver mucinous cystic and intraductal papillary mucinous neoplasms of the bile duct: a case report. *World J Gastroenterol* 2014; **20**: 4102-4105 [PMID: 24744602 DOI: 10.3748/wjg.v20.i14.4102]

17 **Minagawa N**, Sato N, Mori Y, Tamura T, Higure A, Yamaguchi K. A comparison between intraductal papillary neoplasms of the biliary tract (BT-IPMNs) and intraductal papillary mucinous neoplasms of the pancreas (P-IPMNs) reveals distinct clinical manifestations and outcomes. *Eur J Surg Oncol* 2013; **39**: 554-558 [PMID: 23506840 DOI: 10.1016/j.ejso.2013.02.016]

18 **Kato H**, Tabata M, Azumi Y, Osawa I, Kishiwada M, Hamada T, Mizuno S, Usui M, Sakurai H, Isaji S. Proposal for a morphological classification of intraductal papillary neoplasm of the bile duct (IPN-B). *J Hepatobiliary Pancreat Sci* 2013; **20**: 165-172 [PMID: 22426592 DOI: 10.1007/s00534-012-0513-y]

19 **Wan XS**, Xu YY, Qian JY, Yang XB, Wang AQ, He L, Zhao HT, Sang XT. Intraductal papillary neoplasm of the bile duct. *World J Gastroenterol* 2013; **19**: 8595-8604 [PMID: 24379576 DOI: 10.3748/wjg.v19.i46.8595]

20 **Yeh TS**, Tseng JH, Chiu CT, Liu NJ, Chen TC, Jan YY, Chen MF. Cholangiographic spectrum of intraductal papillary mucinous neoplasm of the bile ducts. *Ann Surg* 2006; **244**: 248-253 [PMID: 16858187 DOI: 10.1097/01.sla.0000217636.40050.54]

21 **Paik KY**, Heo JS, Choi SH, Choi DW. Intraductal papillary neoplasm of the bile ducts: the clinical features and surgical outcome of 25 cases. *J Surg Oncol* 2008; **97**: 508-512 [PMID: 18314868 DOI: 10.1002/jso.20994]

22 **Carlos RC**, Branam JD, Dong Q, Hussain HK, Francis IR. Biliary imaging with Gd-EOB-DTPA: is a 20-minute delay sufficient? *Acad Radiol* 2002; **9**: 1322-1325 [PMID: 12449364 DOI: 10.1016/S1076-6332(03)80565-2]

23 **Lee NK**, Kim S, Lee JW, Lee SH, Kang DH, Kim DU, Kim GH, Seo HI. MR appearance of normal and abnormal bile: correlation with imaging and endoscopic finding. *Eur J Radiol* 2010; **76**: 211-221 [PMID: 19545960 DOI: 10.1016/j.ejrad.2009.05.050]

24 **Kim KM**, Lee JK, Shin JU, Lee KH, Lee KT, Sung JY, Jang KT, Heo JS, Choi SH, Choi DW, Lim JH. Clinicopathologic features of intraductal papillary neoplasm of the bile duct according to histologic subtype. *Am J Gastroenterol* 2012; **107**: 118-125 [PMID: 21946282 DOI: 10.1038/ajg.2011.316]

25 **Lee NK**, Kim S, Kim HS, Jeon TY, Kim GH, Kim DU, Park do Y, Kim TU, Kang DH. Spectrum of mucin-producing neoplastic conditions of the abdomen and pelvis: cross-sectional imaging evaluation. *World J Gastroenterol* 2011; **17**: 4757-4771 [PMID: 22147976 DOI: 10.3748/wjg.v17.i43.4757]

26 **Xu J**, Sato Y, Harada K, Yoneda N, Ueda T, Kawashima A, Akishiooi Y. Intraductal papillary neoplasm of the bile duct in liver cirrhosis with hepatocellular carcinoma. *World J Gastroenterol*

2011; **17**: 1923-1926 [PMID: 21528069 DOI: 10.3748/wjg.v17.i14.1923]

27 **Ito K**, Fujita N, Kanno A, Matsubayashi H, Okaniwa S, Nakahara K, Suzuki K, Enohara R. Risk factors for post-ERCP pancreatitis in high risk patients who have undergone prophylactic pancreatic duct stenting: a multicenter retrospective study. *Intern Med* 2011; **50**: 2927-2932 [PMID: 22185981 DOI: 10.2169/internalmedicine.50.6235]

28 **Sohn WJ**, Jo S. A huge intraductal papillary mucinous carcinoma of the bile duct treated by right trisectionectomy with caudate lobectomy. *World J Surg Oncol* 2009; **7**: 93 [PMID: 19961613 DOI: 10.1186/1477-7819-7-93]

29 **Yamashita Y**, Fukuzawa K, Taketomi A, Aishima S, Yoshizumi T, Uchiyama H, Tsujita E, Harimoto N, Harada N, Wakasugi K, Maehara Y. Mucin-hypersecreting bile duct neoplasm characterized by clinicopathological resemblance to intraductal papillary mucinous neoplasm (IPMN) of the pancreas. *World J Surg Oncol* 2007; **5**: 98 [PMID: 17725824 DOI: 10.1186/1477-7819-5-98]

30 **Güllüoglu MG**, Ozden I, Poyanli A, Cevikbas U, Ariogul O. Intraductal growth-type mucin-producing peripheral cholangiocarcinoma associated with biliary papillomatosis. *Ann Diagn Pathol* 2007; **11**: 34-38 [PMID: 17240305 DOI: 10.1016/j.anndiagpath.2006.09.003]

31 **Takanami K**, Hiraide T, Kaneta T, Hayashi H, Unno M, Fujishima F, Fukuda H, Yamada S, Takahashi S. FDG PET/CT findings in malignant intraductal papillary mucinous neoplasm of the bile ducts. *Clin Nucl Med* 2010; **35**: 83-85 [PMID: 20090451 DOI: 10.1097/RLU.0b013e3181c7bff0]

P- Reviewer: dos Santos JS, Li YY, Mansour-Ghanaei F, Kaiser GM, Kumar A, Schofield JB
S- Editor: Ma YJ **L- Editor**: Webster JR **E- Editor**: Ma S

Published by **Baishideng Publishing Group Inc**
8226 Regency Drive, Pleasanton, CA 94588, USA
Telephone: +1-925-223-8242
Fax: +1-925-223-8243
E-mail: bpgoffice@wjgnet.com
Help Desk: http://www.wjgnet.com/esps/helpdesk.aspx
http://www.wjgnet.com

ISSN 1007-9327
9 771007 932045 25>